A first-principles investigation of the solid-state phase transition in the Mo - Fe system

1997 J. Phys.: Condens. Matter 9 5287

(http://iopscience.iop.org/0953-8984/9/24/024)

J. Phys.: Condens. Matter **9** (1997) 5287–5293. Printed in the UK PII: S0953-8984(97)77927-X

A first-principles investigation of the solid-state phase transition in the Mo–Fe system

X Y Huang, J S Pan and Y D Fan

Department of Materials Science and Engineering, Tsinghua University, Beijing 100084, People's Republic of China

Received 18 September 1996

Abstract. The first-principles linear-muffin-tin-orbital method has been applied in studying the two-step phase transition induced by ion mixing in Mo–Fe multilayers which has been observed recently. Three different structures, i.e., cubic $L1_2$, hexagonal $D0_{19}$, and tetragonal $D0_{22}$, of Mo_3Fe have been considered in our study. The results are presented in the form of the total energy as a function of the lattice constant, the cohesive properties, and the density of states for the three structures. In agreement with experiment, the $L1_2$ structure is found to be more stable than either the $D0_{19}$ or $D0_{22}$ structures, which indicates the possibility of a phase transition from the hexagonal close-packed (hcp) to the face-centred cubic (fcc) form. The predicted lattice constants of these two phases fit very well with the experimental ones. The densities of states are also used to analyse the relative stability of different structures in the Mo–Fe system.

1. Introduction

The last two decades have been characterized by a fast development of materials science with special emphasis on the production of new materials. Since the 1980s, both ion mixing (IM) and solid-state reaction (SSR) have been used to study some important problems in physical metallurgy, such as the theories of the alloy phase and phase transformations [1, 2]. Recently, using these two methods, some new metastable crystalline phases and a two-step phase transition were observed in Mo–TM multilayered films (TM refers to Fe, Co, and Ni) [3–5]. These phases have never been found in nature, and have attracted much attention. Their properties and formation mechanism have been studied extensively. Although previous work has been mainly focused on experimental methods for synthesizing them, it is also of great interest to know why these metastable phases can be formed, and what plays the major role in the phase transition induced by IM.

From a theoretical point of view, several approaches are possible. First, one can seek to correlate the crystal structure with significant parameters such as the atomic size, electronegativities, and electron concentration. This was the approach of Hume-Rothery and Coles [6], and Darken and Gurry [7], and this is the line of argument followed by Miedema *et al* [8]. Alternatively, one can attempt to calculate the free energy in order to obtain information by extrapolation from available thermodynamical data [9]. Thirdly, in a more microscopical framework, one can solve the problem exactly by making statistical mechanical calculations as in the cluster variational method [10] or Monte Carlo simulations [11]. Finally, there is the first-principles viewpoint [12]. As efficient and powerful tools, first-principles calculations have been widely used to obtain the electronic structures and cohesive properties of complex systems in their equilibrium states, due

0953-8984/97/245287+07$19.50

to the fast development of computing techniques. Thus, it was inevitable that the first-principles technique would be applied to the study of the solid phase transition induced by IM. However, so far as we are aware, previous theoretical work on phase formations and phase transitions induced by IM and SSR has been mainly based on thermodynamics. Until now, perhaps the most successful model has been that proposed by Alonso *et al* [13], and developed by Zhang and Liu [3]. In their recent work, Zhang and Liu calculated the phase diagrams of some Mo-based alloys, and gave an interpretation of the two-step phase transition induced by IM. Knowledge of the electronic structure of solids is of vital importance for understanding their macroscopic properties on microscopical grounds. However, owing to a lack of first-principles calculations in this area, one cannot achieve an intrinsic understanding of the formation mechanism of these alloys from a microscopical point of view.

It is reported [3] in the literature that two different metastable crystalline phases, i.e., hexagonal $D0_{19}$ and cubic $L1_2$ structures, can be synthesized by IM in Mo_3Fe multilayers, and that the hexagonal structure can change into cubic structure. In this paper, we report a first-principles linear-muffin-tin-orbital (LMTO) study on the phase stability in the Mo_3Fe system. We hoped that this first-principles calculation would prove to give a proper explanation for the two-step phase transition in Fe–Mo multilayers. We have included three different structures in our study, two of which are the observed phases ($D0_{19}$ and cubic $L1_2$); the other is the $D0_{22}$ phase, which is used for comparison. The total energies for these three different structures are calculated, to obtain the more stable crystal structure, as well as the equivalent lattice constant. Besides this, the electronic structure is used to clarify the structure preferences of the metastable phases in the Mo–Fe system.

2. The theoretical method

The total energies and electronic structures of Mo_3Fe with three different structures are obtained by means of the self-consistent tight-binding LMTO (TB-LMTO) method, using the local spin-density (LSD) approximation and the atomic-sphere approximation (ASA) [14, 15]. The von Barth–Hedin exchange–correlation potential is used here [16]. For simplicity, each atom was assumed to occupy the same volume in the unit cell, and hence the identical Wigner–Seitz (WS) radius of these atoms is adopted. It was assumed that the core charge remains unchanged in the formation of the solid from free atoms. Therefore, atomic charge densities were used throughout the calculations. The wave function was expanded in s, p, d orbitals at each atomic site.

From the total energy of the alloy and the constituent elemental solids, one can find the formation energy, using the expression

$$E^{\mathrm{AB}}_{\mathrm{form}} = E^{\mathrm{AB}}_{\mathrm{total}} - [cE^{\mathrm{A}}_{\mathrm{solid}} + (1-c)E^{\mathrm{B}}_{\mathrm{solid}}] \tag{1}$$

where $E^{\mathrm{AB}}_{\mathrm{form}}$ is the total energy per formula unit of the crystalline phase for the equilibrium lattice constants, while $E^{\mathrm{A}}_{\mathrm{solid}}$ and $E^{\mathrm{B}}_{\mathrm{solid}}$ are the total energies of the constituents A and B, respectively. Following this line, the systematic errors in the total energy caused by the use of the ASA can be eliminated effectively. A parabolic fitting to the total energy is adopted to obtain the bulk modulus, since the bulk modulus can be calculated by using the relation

$$B = \Omega \frac{\partial^2 E}{\partial \Omega^2}\bigg|_{\Omega_0} \tag{2}$$

where Ω_0 is the equilibrium volume of the unit cell.

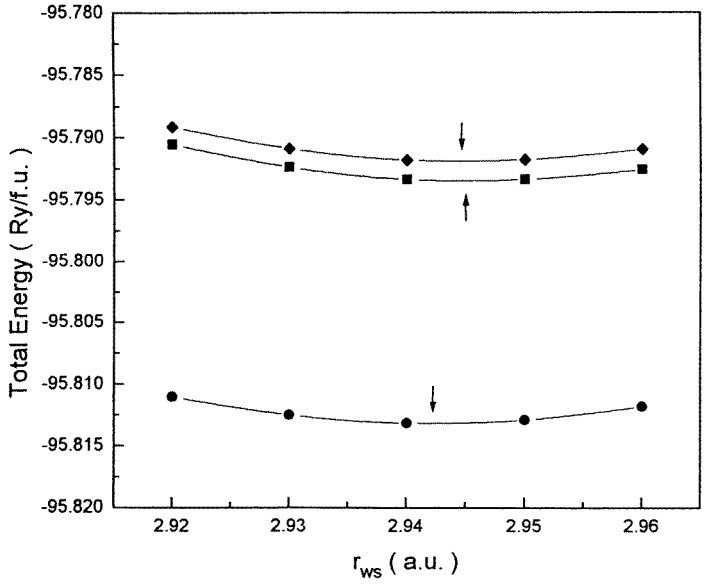

Figure 1. Total energy (Ryd/f.u.) versus the Wigner–Seitz radius r_{WS} (au) of Mo_3Fe with deferent structures. Filled diamonds, filled squares, and filled circles represent the $D0_{19}$, $D0_{22}$, and $L1_2$ structures, respectively.

3. Results and discussion

The total energies are calculated as a function of the Wigner–Seitz radius (r_{WS}) for Mo_3Fe with three different structures, i.e., cubic $L1_2$, tetragonal $D0_{22}$ ($c/a = 2$), and hexagonal $D0_{19}$. The calculated total energies versus r_{WS} are plotted in figure 1. The difference in equilibrium WS radii between any two of these three structures is found to be less than 1%, which implies that the atomic volume effect on the stacking sequence of the ordered close-packed layers is insignificant. From figure 1, one can see that the Mo_3Fe with the $L1_2$ structure has the lowest total energy among the three structures. The total energy difference between the $D0_{19}$ and $L1_2$ structures is 21.4 mRyd/f.u. (f.u. = formula unit), which is much larger than the difference between the $D0_{19}$ and $D0_{22}$ structures. This indicates that the $L1_2$ structure is the most stable structure, and either $D0_{19}$ or $D0_{22}$ may be found as a metastable phase in the ordered Fe_3Mo alloy. This seems reasonable, because it is reported [1] that the hcp + fcc phase can be synthesized in Mo_3Fe multilayers, and can change into a fcc structure under ion irradiation.

The calculated equilibrium cohesive properties of Mo_3Fe with three different structures are listed in table 1. The calculated WS radii for both $L1_2$ and $D0_{19}$ are very close to the experimental ones, with differences of 0.4% and 1.0%, respectively. Note that the formation energies for the three different structures are positive, and hence these ordered phases can be synthesized only as metastable phases through a nonequilibrium process. In order to gain insight into the phase stability from the microscopical point of view, let us check the DOS of Mo_3Fe with the $L1_2$, $D0_{22}$, and $D0_{19}$ structures which are given in figures 2(a), 2(b), and 2(c), respectively. We immediately find an interesting feature in the DOS, i.e., the overall resemblance of the DOS, and nearly the same location of the Fermi level (E_F) for all of these phases. The common feature of the DOS may be demonstrated using the $L1_2$

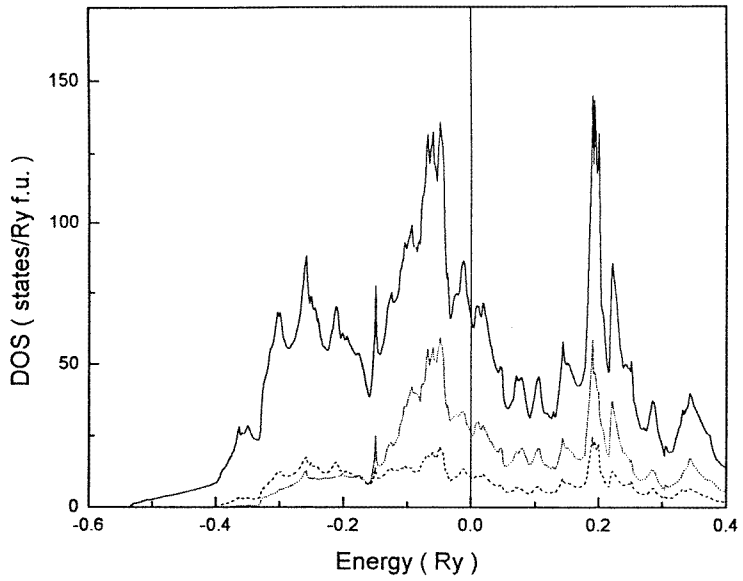

(a)

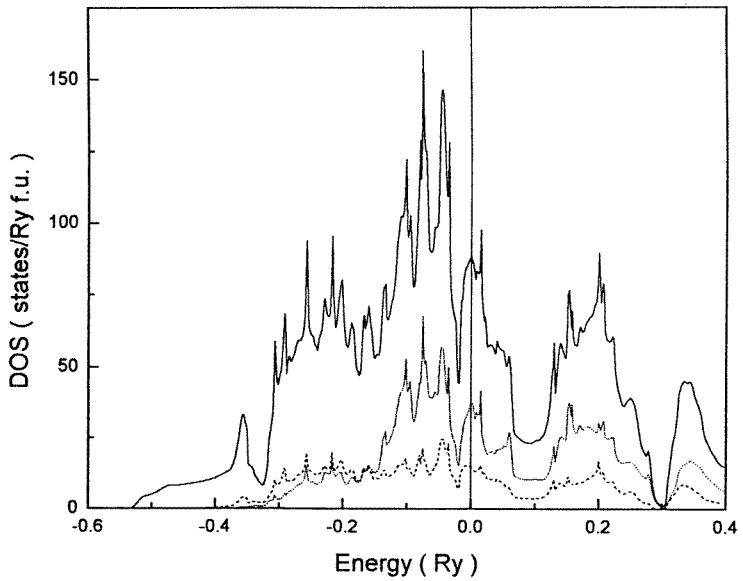

(b)

Figure 2. The total DOS (states Ryd^{-1}/f.u.) and partial d DOS (states Ryd^{-1}/atom) of Mo_3Fe with the (a) $L1_2$, (b) $D0_{22}$, and (c) $D0_{19}$ structures. Solid lines, dotted lines, and dashed lines represent the total DOS, the Fe d states, and the Mo d states, respectively.

structure. One can see from figure 2(a) that the strong hybridization causes the Mo d and Fe d states to overlap over the whole energy range from -0.4 Ryd up to far above E_F. This strong hybridization dominates the cohesion of ordered Mo_3Fe. Figure 3 shows the DOS with three different structures near E_F. It should be noted that in the case of $L1_2$ structure,

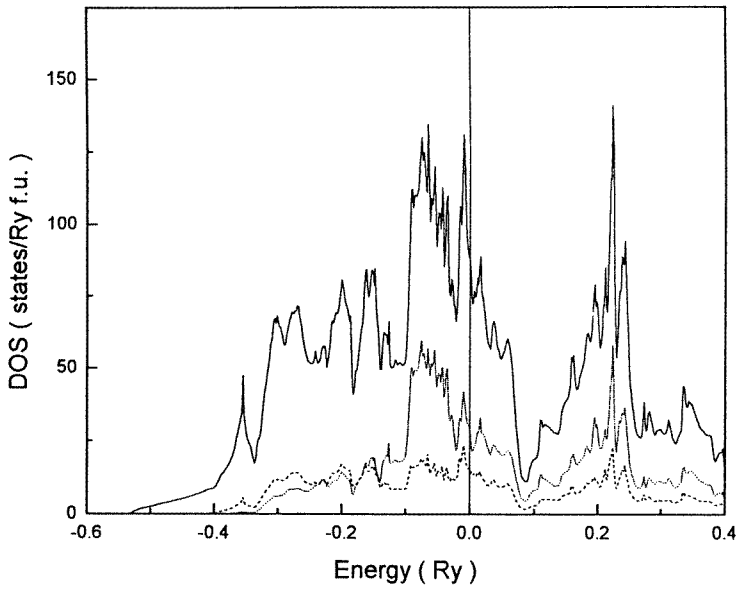

(c)

Figure 2. (Continued)

Table 1. The calculated equilibrium cohesive properties (WS radius r^0_{WS}, bulk modulus B, formation energy E^{AB}_{form}), and the DOS at E_F, for Mo_3Fe with the $L1_2$, $D0_{22}$, and $D0_{19}$ structures.

System	r^0_{WS} (au) Calculated	r^0_{WS} (au) Experimental[a]	B (Mbar)	E^{AB}_{form} (eV/f.u.)	DOS(E_F) (states Ryd^{-1}/f.u.)
Mo_3Fe					
$L1_2$	2.942	2.954	2.86	1.71	65.72
$D0_{22}$	2.945	—	2.95	1.97	88.22
$D0_{19}$	2.945	2.976	2.88	2.00	99.93

[a]Reference [3].

E_F is located in the valley in the bonding area, and corresponds to a lower DOS than that in both the $D0_{22}$ and $D0_{19}$ structures. This leads to a stronger tendency towards structural stability for the $L1_2$ structure for Mo_3Fe. Although it has almost the same value of the DOS at the Fermi level as the $D0_{19}$ structure, the $D0_{19}$ structure shows a stronger tendency towards instability than the $D0_{22}$ structure, due to the existence of the high DOS peak just below E_F.

The partial DOS in figures 2(a), 2(b), and 2(c) show that the Fe d states are predominant in the region below E_F, while the Mo d states are quite uniform on both sides of E_F. Therefore, the valence electrons are transferred from Mo to Fe sites. The charge transfers of Mo_3Fe in the three structures from Mo to Fe sites are listed in table 2. It can be seen that in comparison with the cases for pure bcc Fe and Mo, each Fe atom in the $L1_2$, $D0_{22}$, and $D0_{19}$ structures gains 0.25, 0.24, and 0.23 electrons from the Mo atoms, respectively. It should be noted that the most stable structure corresponds a slightly higher charge transfer

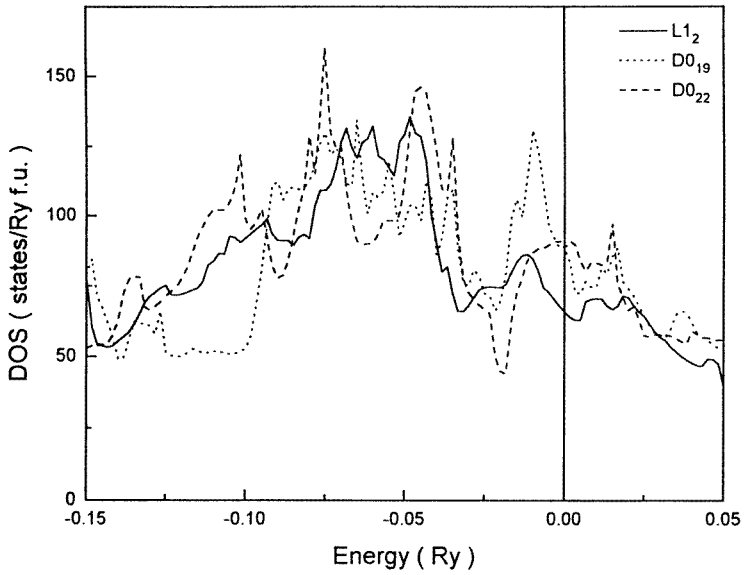

Figure 3. The total DOS (states Ryd^{-1}/f.u.) near E_F for Mo_3Fe with three different structures. Solid lines, dotted lines, and dashed lines represent the $L1_2$, $D0_{22}$, and $D0_{19}$ structures, respectively.

Table 2. The total and partial DOS at E_F, and the number of electrons for metastable phases in Mo_3Fe. N and n represent the DOS at E_F, and the number of electrons, respectively. For comparison, the total and partial DOS at E_F, and the number of electrons in the constituents for bcc Mo and bcc Fe are also listed.

		Atom	N_s	N_p	N_d	N_{tot}	n_s	n_p	n_d	n_{tot}
Mo_3Fe:	$L1_2$	Mo	0.22	1.59	10.40	12.21	0.64	0.67	4.38	5.75
		Fe	0.18	2.81	26.08	29.07	0.81	1.11	6.82	8.74
	$D0_{22}$	Mo	0.18	2.29	14.09	16.56	0.62	0.75	4.39	5.76
		Fe	0.23	2.60	35.71	38.54	0.78	1.12	6.82	8.72
	$D0_{19}$	Mo	0.36	2.64	15.73	18.73	0.64	0.72	4.41	5.77
		Fe	0.22	3.84	28.70	32.76	0.81	1.07	6.82	8.70
Mo:	bcc		0.09	0.99	4.48	5.56	0.66	0.89	4.45	6.00
Fe:	bcc		0.15	0.37	44.06	44.58	0.65	0.80	6.54	8.00

than the other two. This shows that the phase transition from the hcp to the fcc form will cause an extra 0.02 electrons to transfer from Mo to Fe sites.

4. Conclusion

In conclusion, the present self-consistent TB-LMTO total energy calculation has been successfully applied to predict the two-step solid phase transition in the Mo–Fe system induced by IM. Our total energy calculation shows that the Mo_3Fe with the L_{12} structure is the most stable crystalline phase among the three phases. In addition, we have found an inverse relationship between the DOS at the Fermi level and the phase stability.

Acknowledgments

The authors are grateful for useful discussions with Dr Z J Zhang, whose experimental work on IM inspired this study. This work was financially supported by the National Natural Science Foundation of China, and by a computing grant from Cernet High Performance Computing Centre (CHPP).

References

[1] Was G 1989 *Prog. Surf. Sci.* **32** 211
[2] Nastasi M and Mayer J W 1991 *Mater. Sci. Rep.* **6** 1
[3] Zhang Z J and Liu B X 1995 *J. Phys. C: Solid State Phys.* **7** L293
[4] Zhang Z J and Liu B X 1994 *J. Appl. Phys.* **76** 3351
[5] Liu B X, Zhang Z J and Bai H Y 1993 *J. Non-Cryst. Solids* **156** 603
[6] Hume-Rothery W and Coles B R 1965 *Atomic Theory for Students of Metallurgy* 5th edn (London)
[7] Darken L S and Gurry R W 1953 *Physical Chemistry of Metals* (New York: McGraw-Hill)
[8] Miedema A R, de Chatel P F and de Boer F R 1980 *Physica* **100** 1
[9] Kaufman L 1989 *Alloy Phase Stability* vol 163, ed G M Stocks and A Gonis (Dordrecht: Kluwer Academic) pp 145–76
[10] Connolly J W D and Williams A R 1983 *Phys. Rev.* B **27** 5169
[11] Binder K 1979 *Monte Carlo Methods in Statistical Physics* 2nd edn (Berlin: Springer)
[12] Andersen O K, Jepsen O and Glötzel D 1985 *Highlights of Condensed-Matter Theory* ed F Bassani, F Fumi and M P Tosi (New York: North-Holland) p 59
[13] Alonso J A, Gallego L J and López J M 1988 *Phil. Mag.* A **58** 79
[14] Andersen O K 1975 *Phys. Rev.* B **12** 3060
[15] Skriver H L 1984 *The LMTO Method: Muffin-Tin Orbitals and Electronic Structure* (New York: Springer)
[16] von Barth U and Hedin L 1972 *J. Phys. C: Solid State Phys.* **5** 1629